Progress In Electromagnetics Research, Vol. 137, 599–619, 2013

BROADBAND MODIFIED RECTANGULAR MICROSTRIP PATCH ANTENNA USING STEPPED CUT AT FOUR CORNERS METHOD

Alishir MoradiKordalivand* **and Tharek A. Rahman**

Wireless Communication Centre, Faculty of Electrical Engineering, Universiti Teknologi Malaysia, Skudai, Johor 81310, Malaysia

Abstract—In this paper, a new method that called the "Stepped Cut at Four Corners" is introduced to design a multi-mode/broadband modified rectangular microstrip patch antennas (MRMPAs). In order to become acquainted with the new method, the design process of a monopole broadband MRMPA suitable for multifunctional wireless communication bands is explained. The methodology of the proposed broadband MRMPA design is presented in six stages. The first stage is designing a single-mode RMPA. Subsequently, by creating a step at the corners using the proposed method a dual-mode antenna is obtained at the second stage, while the triple-mode and multi-mode antennas are designed, at the third and fourth stages respectively. Two types of broadband antennas are obtained, the stepped line and straight line antennas. By increasing the number of steps, the antenna's operating bandwidth (BW), with return loss less than −10 dB, covers the frequency range from 900 MHz to 2.6 GHZ, which is suitable for GSM (900 MHz and 1.5 GHz), WiFi (2.4 GHz) and LTE (2.6 GHz) applications. In addition, the antenna prototype has been fabricated and measured in the all stages, in order to validate the simulation results, and there is a close agreement between the simulated and measured results.

1. INTRODUCTION

Antennas are very significant in the area of wireless communications, and the microstrip patch antenna (MPA) is one of the most popular and widely used in this field. Indeed, the MPAs have attracted so much research interest, due to their light weight, compatibility,

Received 17 January 2013, Accepted 28 February 2013, Scheduled 7 March 2013

* Corresponding author: Alishir Moradikordalivand (alimoradi2020@gmail.com).

low-profile, ease of fabrication, and low cost. Other merits include ease of integration with other kinds of microwave integrated circuits (MICs) on the same substrate and capability of being deployed for both linear and circular polarizations. However, MPAs have such disadvantages as low power handling capability, low gain, and narrow BW. MPAs comprise narrow BW that is approximately 1–5%, which is the most major limiting factor for its widespread applications. Most of the previous contributions in this research area were to increase the BW of MPAs [1, 2], and therefore, several measures have been introduced to achieve this objective, including modified shape patches, which is a method of modifying the shape of patch [3–8], utilization of slotted ground structure [9–13], modification of rectangular and circular patches to rectangular [14] and circular rings [15, 16]. Another method includes an impedance matching network method proposed to enhance the MPAs BW [17–19]. Several parasitic patches, such as shorted quarter-wavelength, rectangular patches and narrow strips, are used as gap-couple to the central-fed rectangular patch in planar multiresonator structure [20–26]. With different layers of the dielectric substrate, two or more patches are stacked on one another in the multilayer configuration, which is categorized as electromagnetically aperture-coupled or coupled MPAs as regards to the coupling mechanism [27–30]. The stacked and planar multiresonator techniques are combined with the proposed method to increase the BW and the gain of the stacked multiresonator MPAs. A circular patch on the bottom layer or probe-fed single rectangular patch has been used to excite circular patches on the top layer or multiple rectangular, respectively [31–33]. Another method to enhance the BW is LC method, which distributes LC circuit on the backside of the conventional patch antenna [34].

In this paper, the "Stepped Cut at Four Corners" method for designing a monopole multi-mode/broadband MRMPA has been proposed based on modifying the patch shape. In order to become acquainted with the new method, we will describe the design procedure, simulation, and fabrication of a broadband MRMPA with operating frequency from 900 MHZ to 2.6 GHz. The proposed MRMPA covers GSM (900 MHz and 1.5 GHz), Wi-Fi (2.4 GHz) and LTE (2.6 GHz) applications.

2. RMPAs MODEL

Figure 1 shows the RMPA configuration, including a dielectric substrate located between a radiating patch and a ground plane. Generally, the patch is prepared of conducting material such as gold

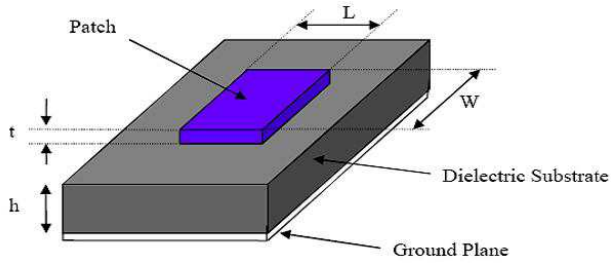

Figure 1. Structure of RMPA.

or copper in any shape. On the dielectric substrate, the feed lines and radiating patch are usually photo-etched [35, 36].

The microstrip patch antenna analysis is represented by some models such as the transmission line model, cavity model, full wave model and characteristic mode. The cavity model is more accurate and gives a good physical insight thus very complex compared to the transmission line model that is the simplest of all models and less accurate. The characteristic mode is typically performed on electrically small to intermediate size antennas for simplicity [37, 38]. However, the full wave model is the most accurate and complex of the models and can analyze single elements, arbitrary shaped elements and infinite antenna arrays.

The transmission line model is used in this work because of its simplicity to implement and its output good performance in antenna designs in terms of efficiency and return loss and also it is well suited for RMPAs design. By choosing operating frequency f_r and a substrate with the required permittivity ε_r, and also defining the substrate thickness h, the design starts. Based on the transmission line model, the length L and width W of the patch are calculated as:

$$W = \frac{v_0}{2f_r}\sqrt{\frac{2}{\varepsilon_r + 1}} \tag{1}$$

$$L = \frac{v_0}{2f_r\sqrt{\varepsilon_{reff}}} - 2\Delta L \tag{2}$$

where, v_0 is the speed of light in free space, ε_{reff} the effective permittivity, and $2\Delta L$ the extension in length due to fringing effects:

$$\varepsilon_{reff} = \frac{\varepsilon_r + 1}{2} + \frac{\varepsilon_r - 1}{2}\left[1 + 12\frac{h}{W}\right]^{-1/2} \tag{3}$$

$$\Delta L = 0.412h\frac{(\varepsilon_{reff} + 0.3)\,(W/h + 0.264)}{(\varepsilon_{reff} - 0.258)\,(W/h + 0.8)} \tag{4}$$

Although the patch design is simple, feeding design mechanism is not direct. There are four main methods used to design the feed, which are probe feed, microstrip-line feed, Proximity-coupled feed and aperture-coupled feed. However, we used a microstrip-line feed because of the simplicity of the model, fabrication and match [35, 36].

3. CONCEPT OF STEPPED CUT AT FOUR CORNERS METHOD

The proposed method, called the "Stepped Cut at Four Corners (SCFC)" is used to design of Multimode/Broadband MRMPAs. As the name implies, four corners of the rectangular patch are cut to create the desired BW by the stepped approach which will be explained in the following text. Firstly, in the proposed method, the lower cutoff frequency (FL) and upper cutoff frequency (FH) must be determined in order to specify the BW range. Next, the values of the patch's length and width will be determined for the excited frequencies of FH and FL, using Transmission Line equations, given in Equations (1)–(4). According to obtained patch's dimensions, the patch of FL is bigger than that of FH. Therefore, the coordinate positions of FH patch are inserted within coordinate positions of that of the FL. Considering the nested structure of the patches, it can be seen that they are all concentric, for example, the point (0, 0); and they are placed on the x-y plane of the coordinate system. As mentioned earlier, the patch obtained from FL is the largest in terms of dimensions; therefore it is considered as the main patch.

As can be seen in Figure 2, the rectangles with red and green colour lines are the patches designed for the FL and FH respectively. W_L and L_L denote the FL patch length and width, respectively. Also the corresponding FH patch width and length are W_H and L_H. Each design covers only one operating frequency, thus if a broadband design is expected from FL to FH frequency range, all of the frequencies within the BW must be covered. Therefore, the length and width of the patches must be from L_L to L_H and W_L to W_H, respectively. As shown in Figure 2, the patch obtained from FH is shown in white colour; however the patch colour becomes darker as it moves toward FL. In Figure 2, by drawing the lines from internal patch corners (designed for FH patch and displayed in green colour) toward external patch lines (designed for FL patch and displayed in red colour), step cutting position is specified in each corner, which are shown in blue colour. The width and length of the patches within the given BW, denoted by F1 to Fn-1 are drawn from W_1 to W_{n-1} and L_1 to L_{n-1}, respectively. In order to connect F1-Fn-1 patches to FL patch for creating the steps

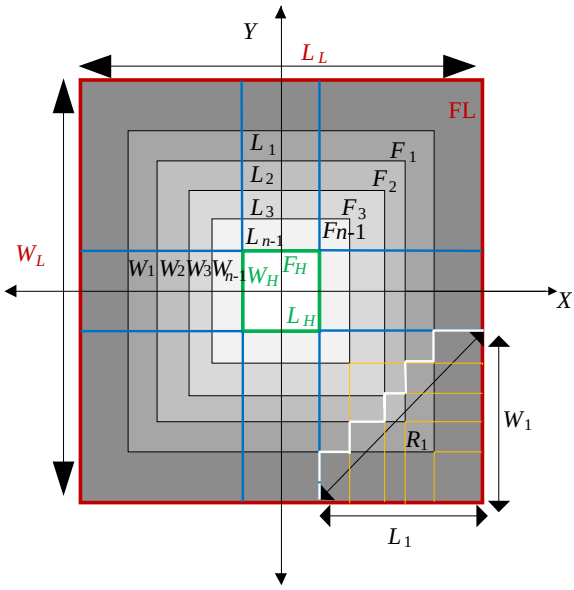

Figure 2. Configuration position of the patches in the SCFC method.

at the corners, a process similar to the one mentioned above is followed. By referring to Figure 2, it is shown that a grid plane with $1/n$ spacing is created at the corners, where n is the number of the patches designed inside the main patch. Figure 3 shows geometric details of the corners in this method. In order to calculate the dimensions of the first step at the corners, the length and width relate to L_1 and spacing between the coordinate position of W_{FL} and W_{F1}. Second step width is considered from the distance between the coordinate position of W_{F1} and W_{F2}, and length is related to the distance between the coordinate position of L_{FL} and L_{Fn-1} and other steps created in the same process. The step path created using this method is shown in white colour. By creating each step, in fact an excited resonant frequency is created over the BW therefore by increasing the number of steps; the excited resonant frequencies are increased as long as the BW is covered.

Whereas the patch height (t) is extremely thin compared to its width and length, z-axis are ignored in coordinating system and all calculations are done on the x-y plane. To obtain the dimensions and coordinate position of the patches length and width over the BW, following equations are used in accordance with Figure 3.

$$W_1 = \frac{W_L - W_H}{2} = \sum_{n=1}^{n=n} W_{Rn} \tag{5}$$

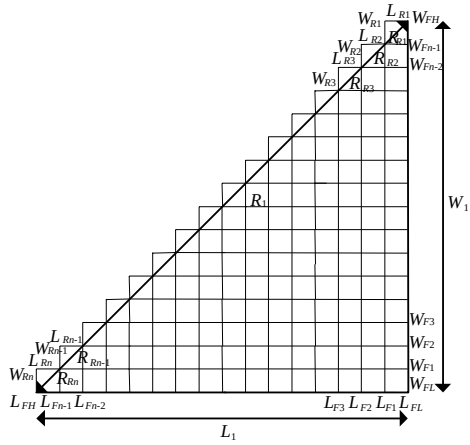

Figure 3. Geometric details of steps at the corners.

$$L_1 = \frac{L_L - L_H}{2} = \sum_{n=1}^{n=n} L_{Rn} \tag{6}$$

When the steps dimension are same:

$$W_R = W_{R1} = W_{R2} = \ldots = W_{Rn} \text{ and } L_R = L_{R1} = L_{R2} = \ldots = L_{Rn}$$

$$W_R = \frac{W1}{n} \tag{7}$$

$$L_R = \frac{L1}{n} \tag{8}$$

$$R_1 = n \times \sqrt{L_R^2 + W_R^2} \tag{9}$$

where, n is the number of steps, R_1 the stepped path, and W_R and L_R are the width and length of step, respectively. Otherwise:

$$\{W_{Rn}(n)\} = \left\{ \begin{matrix} W1 & n = 1 \\ W_{Fn-1} - W_{Fn} & 2 \leq n < \infty \end{matrix} \right\} \tag{10}$$

where, $W_{FH} = W_{Fn}$, $W_{FL} = W_{F0}$, W_{F1} to W_{Fn-1} are patches width position on the y-axis and W_{R1}–W_{Rn} are step width.

$$\{L_{Rn}(n)\} = \left\{ \begin{matrix} L1 & n = 1 \\ L_{Fn-1} - L_{Fn} & 2 \leq n < \infty \end{matrix} \right\} \tag{11}$$

where $L_{FH} = L_{Fn}$ and $L_{FL} = L_{F0}$.

$$R_{Rn} = \sqrt{L_{Rn}^2 + W_{Rn}^2} \tag{12}$$

$$R_1 = \sum_{n=1}^{n=n} R_{Rn} = \sqrt{L_{R1}^2 + W_{R1}^2} + \sqrt{L_{R2}^2 + W_{R2}^2} \ldots + \sqrt{L_{Rn}^2 + W_{Rn}^2}$$
$$= \sum_{n=1}^{n=n} \sqrt{L_{Rn}^2 + W_{Rn}^2} \quad (13)$$

where, L_{F1} to L_{Fn-1} are patches length position on the x-axis, and $L_{R1} - L_{Rn}$ are steps length.

When n is larger, the number of steps created at the corners is more, and R_1 becomes almost linear and acts somehow as hypotenuse of a right triangle with sides of W_1 and L_1. The values of R_1 can be obtained by the following equation:

$$R_1 = \sqrt{L_1^2 + W_1^2} \quad (14)$$

As explained in this section, multi-mode/broadband MRMPAs can be designed very quickly using simple equations.

4. DESIGN PROCESS OF PROPOSED BROADBAND MRMPA USING SCFC METHOD

In order to become familiar with SCFC method, the design process of monopole broadband MRMPA with frequency range from 900 MHz to 2.6 GHz is explained. This design can be used for GSM (900 MHz/1.5 GHz), WiFi (2.4 GHz) and LTE (2.6 GHz) applications. All designs and simulations of the RMPAs with the proposed method are done using CST Microwave Studio software. FR-4 dielectric substrate with relative permittivity $\varepsilon_r = 4.3$, thickness $h = 1.6$ mm, Length L_s =90 mm and width $W_S = 130$ mm is used. Radiating patch and ground plane are on the top and bottom of the dielectric substrate, respectively and made of copper material with thickness $t = 0.035$ mm and conductivity $\sigma = 5.96e^7$ s/m. The ground plane length and width are $L_G = 18$ mm and $W_G = 90$ mm, respectively and remain constant in all stages of the design process. To achieve 50 Ω output impedance matching with the SMA connector, a transmission line fed with width $W_F = 3$ mm and length $L_F = 20$ mm was used. The following explains the design process of the proposed broadband MRMPA.

4.1. Stage I: Single-mode RMPA

As explained in Section 3, dimensions of patches at the lowest frequency (FL = 900 MHz), the highest frequency (FH = 2.6 GHz) as well as desired frequencies between FL and FH must be obtained from Equations (1)–(4). Table 1 gives the dimensions for patches in

the frequency range 0.9–2.6 GHz with Step 100 MHz. In this stage, a single-mode RMPA for an excited resonant frequency at FL = 900 MHz is proposed. Figure 4 shows the prototype photographs and geometric details of the single-mode RMPA. By referring to Table 1, it is clear that width $W_L = 102$ mm and length $L_L = 80$ mm obtained for this patch have the largest dimensions, thus this patch is considered as the main patch.

Table 1. Dimensions of patches in frequencies range 0.9–2.6 GHz with step100 MHz.

Freq. (GHz)	0.9	1	1.1	1.2	1.3	1.4	1.5	1.6	1.7
W (mm)	102	92	84	76	71	66	61	56	54
L (mm)	80	72	65	60	55	51	47	44	42
Freq. (GHz)	1.8	1.9	2	2.1	2.2	2.3	2.4	2.5	2.6
W (mm)	51	48.5	46	44	42	40	38	36	35
L (mm)	40	38	36	34	32.5	31	29.5	28	27

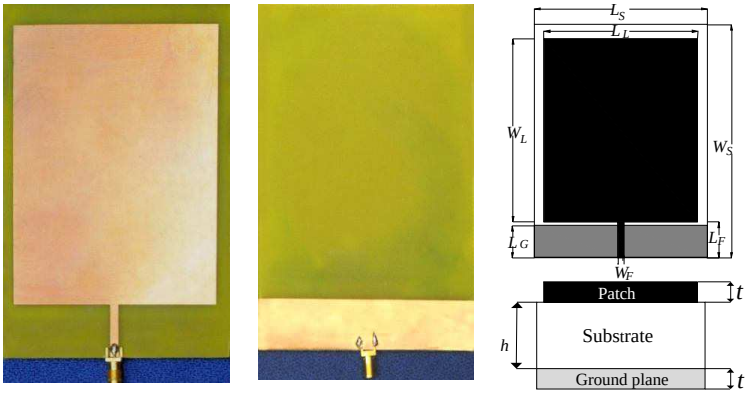

Figure 4. Photographs of fabricated prototype and Geometric details of single-mode RMPA. (a) Front view. (b) Back view. (c) Top & side view.

4.2. Stage II: Dual-mode MRMPA

According to Table 1, it can be seen that the values of width and length for the patch at $F_H = 2.6$ GHz are the smallest. By referring to SCFC method, $L_H = 27$ mm and $W_H = 35$ mm in term of coordinate

positions are within and concentric with the main patch in x-y plane of the coordinate system. At this stage using Equations (10) and (11), step length and width at each corner are found to specify the BW. Pictures of fabricated antenna and configuration for arrangement of patches as well as specifications of the step created at the corners (shown with hachure) are indicated in Figure 5. By removing the hachured sections from main patch, in fact two excited resonant frequencies at FL = 900 MHz and FH = 2.6 GHz are obtained, and the designed antenna acts as dual-mode, as expected.

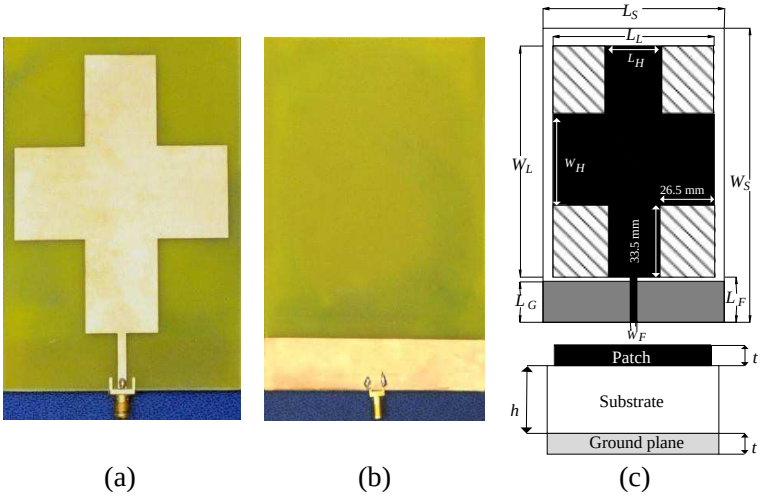

Figure 5. Pictures of fabricated prototype and configuration details of dual-mode MRMPA. (a) Front view. (b) Back view. (c) Top & side view.

4.3. Stage III: Triple-mode MRMPA

To design the triple-mode MRMPA according to the CSFC method, two steps must be created in each corner of the main patch. By creating a patch within frequency range patches from F_L to F_H, in fact helps to create the third excited resonant frequency. The width and length coordinate position of new patch is obtained using Equations (1)–(4) that within W_L to W_F and L_L to L_F, respectively. The middle patch, same as FL patch, is concentric with the main patch in x-y plane of the coordinate system and related to frequency of 1.5 GHz according to Table 1. Figure 6 illustrates the photos of fabricated prototype of proposed antenna and structural configuration for the arrangement of

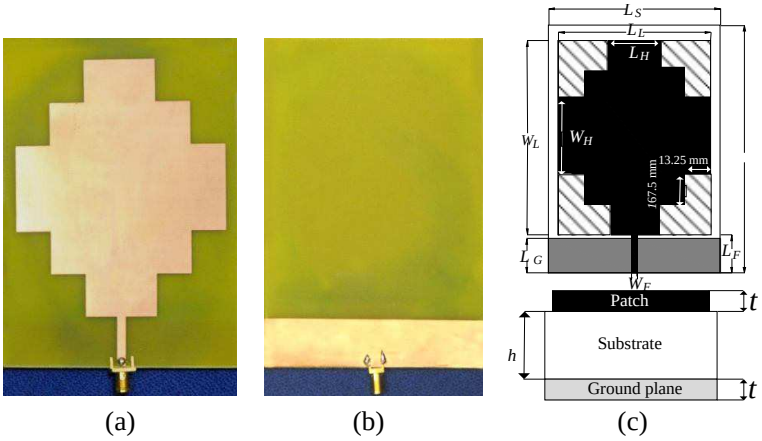

Figure 6. Photos of manufactured prototype and structural details of Triple-mode MRMPA. (a) Front view. (b) Back view. (c) Top & side view.

the patches as well as specifications of the steps created at the corners of the main patch. As shown in Figure 6, if the hachured section is removed from the main patch, three excited resonant frequencies will be resulted at F_L =900 MHz, $F_1 = 1.5$ GHz and FH = 2.6 GHz.

4.4. Stage IV: Multi-mode MRMPA

In order to show details of the design towards achieving multimode antenna, the number of steps at main patch corners are increased using CSFC method. Three patches are created in frequency ranges from FL to FH with appropriate distances and concentric with the main patch in x-y plane of the coordinate system. By increasing the steps, the number of excited resonant frequencies in the specified part of the BW are enhanced; therefore a multimode antenna is obtained. Figure 7 shows a detailed geometric structure and pictures of front and back view of fabricated prototype obtained at this stage. In the figure, some parts of the patch corners are specified by hachure which is removed from the main patch to achieve the multi-mode MRMPA. Considering the results obtained from stage two to four, it is shown that broadband MRMPA is gradually realized in the expected frequency range.

4.5. Stage V: Broadband MRMPA with Stepped Line

In the previous stage, it was observed that using CSFC method, the designed MRMPA was transformed into multi-mode from single mode. As explained in Section 3, $n - 1$ patches can be created between

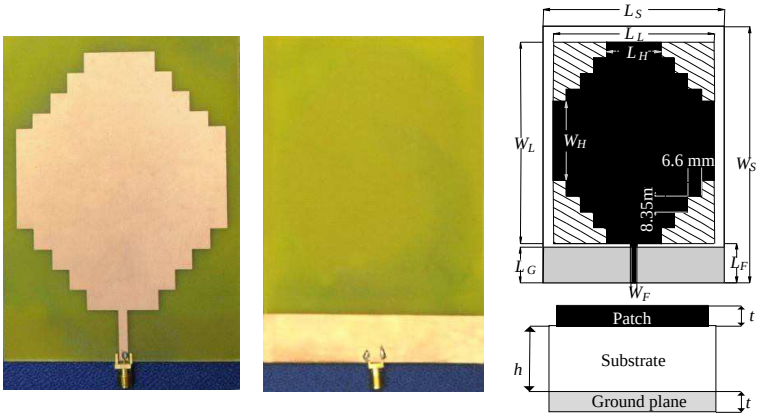

Figure 7. Photographs of manufactured prototype and geometric details of multimode **M**RMPA. (a) Front view. (b) Back view. (c) Top & side view.

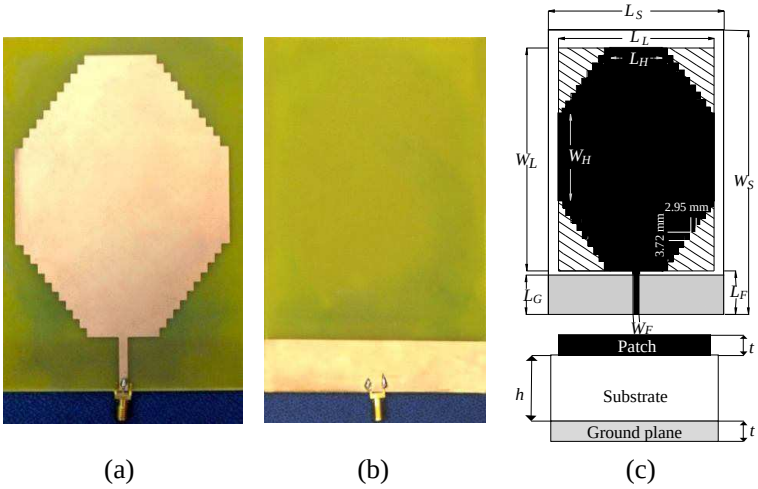

Figure 8. Photographs of fabricated prototype and geometric details of broadband MRMPA using stepped line. (a) Front view. (b) Back view. (c) Top & side view.

frequencies ranging from FL to FH, which create n steps at each corner of main patch. For designing the expected broadband MRMPA with full coverage of the BW, the number of steps at the corners using the SCFC method has increased. As shown in Figure 8, ten steps are created at the corners of the main patch for ensuring full coverage of

the BW by the antenna. It is observed from the obtained results that specifications of the antenna, such as return loss, gains, are improved by increasing the number of steps at the corners. Figure 8 also shows photographs of manufactured prototype and geometric details related to created stepped path and removed parts of the main patch.

4.6. Stage VI: Broadband MRMPA with Straight Line

By increasing the number of steps at the corners, in fact the number of the exited resonance frequencies over the impedance BW is investigated. There are infinite frequencies between F_L to F_H. If the number of steps at the corners increases infinitely, the steps become smaller and reach a point that the step path (R_1) acts as a line with infinite points. By calculating W_1 and L_1 using Equations (10) and (11), R_1 acts as hypotenuse in a right triangle with W_1, L_1 sides, which can be calculated using Equation (14). Figure 9 shows the geometric details and photos of fabricated proposed broadband MRMPA.

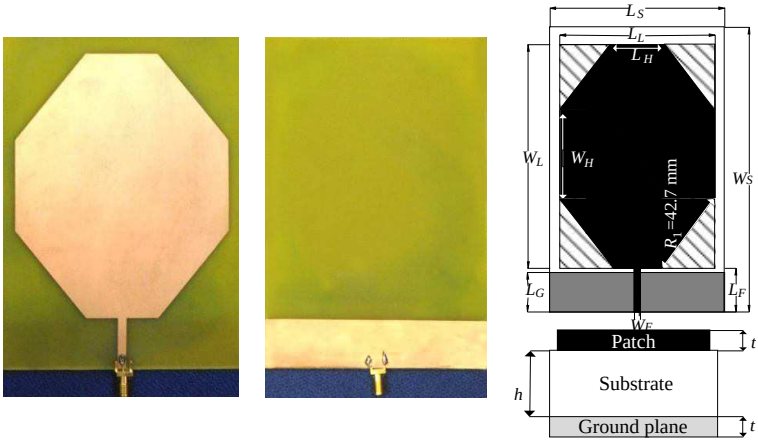

(a) (b) (c)

Figure 9. Photos of fabricated prototype and geometric details of Broadband MRMPA proposed using straight line. (a) Front view. (b) Back view. (c) Top & side view.

5. SIMULATION AND MEASUREMENT RESULTS

In order to validate the simulated results obtained from CST Microwave Studio software, the prototype has been fabricated and measured by Rohde and Schwarz ZVL Network analyzer at all stages of

the proposed RMPAs. Simulated vector surface current distributions in radiating patch and simulated and measured return losses are depicted in Table 2.

Comparison between the simulation and measurement return losses (RL) results is illustrated in Table 2, as it can be seen approximately that there is a good agreement between the results at all stages. The first stage related to the proposed single-mode RMPA for operating frequency at 900 MHz, whose approximate return loss −12-dB was obtained from both simulation and measurement. The second stage demonstrates a dual-mode MRMPA using CSFC method for two exited resonance frequencies at FL = 900 MHz and FH = 2.6 GHz. Consequently, return losses −27 dB and −17 dB for operating frequencies at FL and FH were obtained, respectively. Stage III proposes a triple-mode MRMPA. As expected, three exited resonance frequencies at 900 MHz, 1.5 GHz and 2.6 GHz were obtained. For these frequencies, it can be seen from Table 2 that return loss values are −28 dB, −27 dB and −16 dB for simulation and −16 dB, −25 dB and −13 dB for measurement, respectively. In stage IV, by increasing the number of steps at the corners using SCFC method, a multi-mode MRMPA was obtained. By referring to results, there are desired results based on the return loss less than −10 dB across frequency bands from 900 MHz to 1.65 GHz and 2.25 GHz to 2.6 GHz. In stage V to cover entire BW by proposing MRMPA, the number of steps is enhanced and stepped line is created at the corners. Considering the results obtained at stage V, it can be observed that the designed MRMPA has a broadband performance from 900 MHz to 2.6 GHz based on $RL < -10$ dB that provides the approximately stable omnidirectional/bidirectional radiation pattern over the BW; therefore the whole expected BW using SCFC method was covered. In the last stage, assuming an infinite number of steps at the corners, the stepped line became a straight line. In this stage, the proposed MRMPA produced approximately similar results as obtained in stage V but the difference is the stepped line model gives results that are adjustable in the range of the BW by changing the dimensions of the steps whereas in the straight line model all results remains fixed.

Figures 10 and 11, illustrate simulated and measured return losses of RMPAs at all stages, respectively. According to the figures, the evolution process from single-mode to broadband MRMPA can be seen. The desire frequency band is specified by highlight. Therefore, it is clear that the diagrams of broadband MRMPAs have covered the entire BW.

Stable omnidirection at the lower frequencies and approximate bidirection at the upper frequencies have been achieved for the far

Table 2. Simulated and measured return loss and vector surface current distributions of RMPAs.

Structure	Surface current	Return loss
Stage I: Single mode	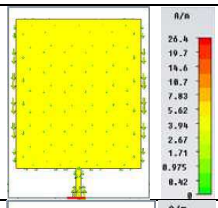	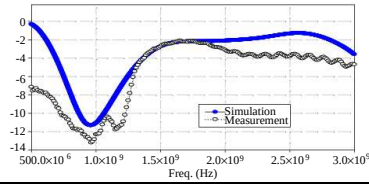
Stage II: Dual mode	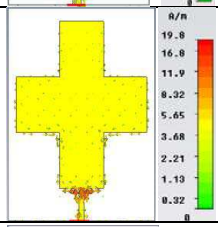	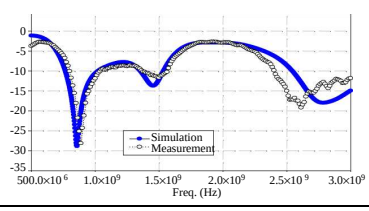
Stage III: Triple mode	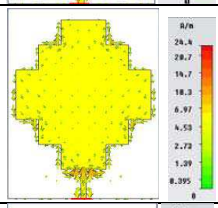	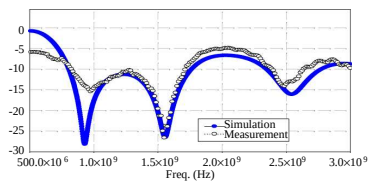
Stage IV: Multi mode	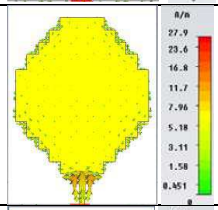	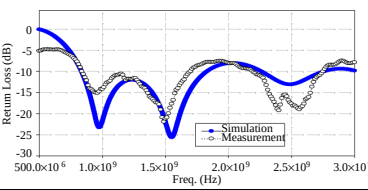
Stage V: Broadband stepped line	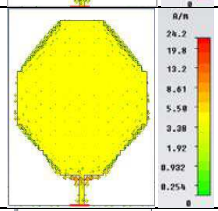	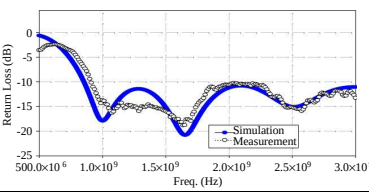
Stage VI: Broadband straight Line	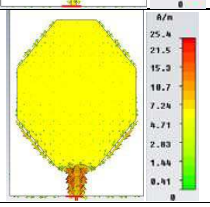	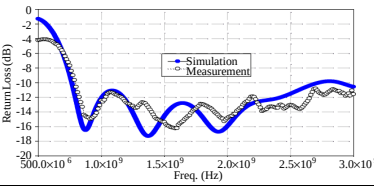

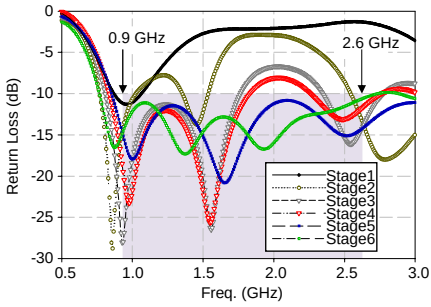

Figure 10. Simulated return loss of the RMPAs.

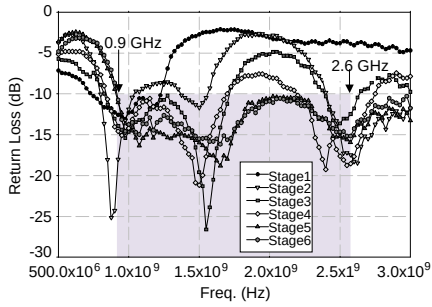

Figure 11. Measured return loss of the RMPAs.

field radiation pattern of proposed monopole broadband MRMPA over the BW. The maximum radiated field directs in the direction of $+z$ and $-z$, for the desired direction. Figure 12 shows the simulated normalized E and H-plane radiation patterns of proposed broadband MRMPA for resonant frequencies at 900 MHz, 1.5 GHz, 2.4 GHz and 2.6 GHz. Figure 12(a) shows, a linear polarization with the broadside and bidirectional E-plane radiation pattern and almost omnidirectional H-plane radiation pattern at 900 MHz operating frequency. Figure 12(b), (c) and (d), show both E and H-plane radiation pattern of operating frequencies at 1.5 GHz, 2.4 GHz and 2.6 GHz, that polarization at these frequencies from linear to circular and radiation patterns approximately bidirectional, respectively. It is found that the radiation pattern in E-plane tilts from z axis, and the main lobes spread to four directions with 45 degree from the z axis. As mentioned in Section 3, the lowest and highest frequencies over the BW belong to the biggest and smallest dimension of the patch, respectively. Therefore, by decreasing the dimension of the patch and the corners, the radiation pattern has changed at the upper frequencies. It is observed from Figure 13 that axial ratios of the proposed broadband MRMPA at upper frequencies of desire BW are below 3 dB, thus polarization is circular.

The vector surface current distributions in the radiation patch at the operating frequency (stage I: 900 MHz, stages II–VI: 2.6 GHz) are shown in Table 2. It can be seen that at all stages except stage I there is the most surface current distribution on the stepped line path. This means that the maximum surface current density at the corners is due to the operating frequencies via the steps size.

Furthermore to the radiation characteristics, the realized gains of the proposed RMPAs are shown in Figure 14. In accordance with the

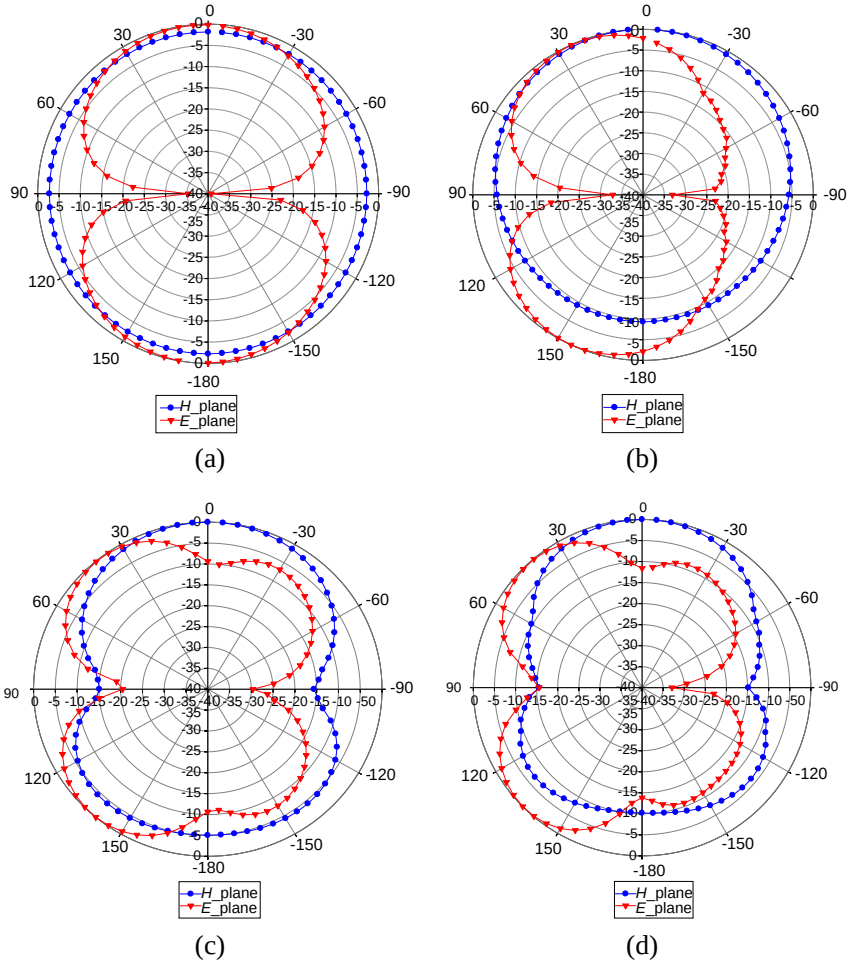

Figure 12. Simulated radiation patterns of the broadband MRMPA. (a) 0.9 GHz, (b) 1.5 GHz, (c) 2.4 GHz, and (d) 2.6 GHz.

results, by increasing the number of steps at the corners the gains enhanced correspondingly, along the frequency band. Consequently at the design stage of the proposed broadband MRMPA, gains of 2.6–4.6 dBi are achieved at the desired direction ($\theta = 0^{\circ}$ and $\varphi = 90^{\circ}$) over the BW.

Figure 15 shows the radiation efficiency simulated of the proposed RMPAs at the all stages. By referring to the figure, it is observed that the radiation efficiency of proposed broadband MRMPAs is more

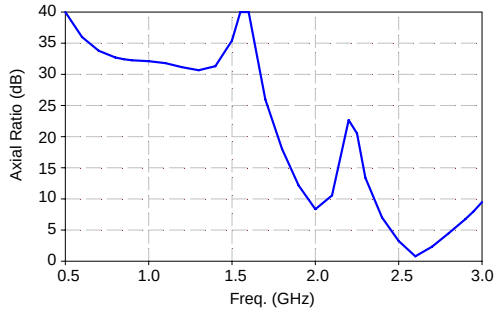

Figure 13. Axial Ratios of proposed broadband MRMPA.

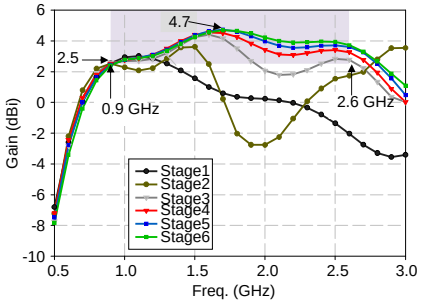

Figure 14. Simulated realized gain of the RMPAs.

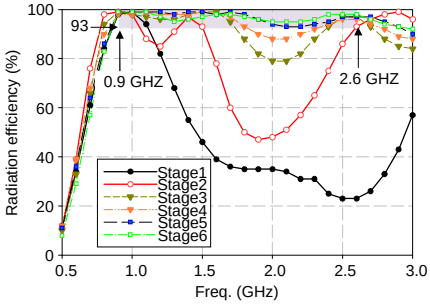

Figure 15. Simulated Radiation efficiency of the RMPAS.

than 93% across the whole BW that is highlighted and specified by blue and green colour diagrams that are belonging to stages V and VI, respectively.

6. CONCLUSION

A new method, "Stepped Cut at Four Corners", for designing a multi-mode/broadband MRMPAs, has been proposed in this paper. In order to become familiar with the proposed method, the process of designing a broadband MRMPA has been analyzed. The proposed broadband MRMPA is suitable for multifunctional wireless communication systems. The design process includes six stages, starting from designing a single-mode RMPA with a resonant frequency of 900 MHz and developed to design a Dual-mode, Triple-mode, Multi-mode and finally the expected broadband MRMPA for operating frequency band from 900 MHz to 2.6 GHz. Complete measurements

were carried out at each stage of the design, in order to validate the simulation results with the measured ones. Each of the stages discussed in details the methodology of creating the steps at the patch's corners to enhancing the impedance BW. The proposed broadband MRMPA can be used for GSM (900 MHz and 1.5 GHz), WiFi (2.4 GHz) and LTE (2.6 GHz) applications. The RMPAs have demonstrated good performance in terms of return loss, radiation pattern, gain and efficiency. The simulated gains were obtained as 2.6–4.7 dBi at the desired direction. In addition, the radiation efficiency was more than 93% with a return loss below −10 dB over the BW. It is found that the measurement and simulation results are in close agreement. It should be noted that some reasons for using SCFC method are simplicity of calculating the steps dimensions for expected resonance frequencies, the capability to design all types of multi-mode/broadband MRMPAs and ability to change the polarization of the antenna from linear to circular.

REFERENCES

1. Milligan, T. A., *Modern Antenna Design*, John Wiley & Sons, Inc., Hoboken, New Jersey, 2005.
2. Kumar, G. and K. P. Ray, *Broadband Microstrip Antennas*, Artech House, Boston, 2003.
3. Islam, M. T., M. N. Shakib, and N. Misran, "Broadband E-H shaped microstrip patch antenna for wireless systems," *Progress In Electromagnetics Research*, Vol. 98, 163–173, 2009.
4. Pouyanfar, N. and S. A. Rezaeieh, "Compact UWB antenna with inverted hat shaped resonator and shortening via pins for filtering properties," *Progress In Electromagnetics Research Letters*, Vol. 33, 187–196, 2012.
5. Abbaspour, M. and H. R. Hassani "Wideband star-shaped microstrip patch antenna," *Progress In Electromagnetics Research Letters*, Vol. 1, 61–68, 2008.
6. Xu, H.-Y., H. Zhang, K. Lu, and X.-F. Zeng, "A holly-leaf-shaped monopole antenna with low RCS for UWB application," *Progress In Electromagnetics Research*, Vol. 117, 35–50, 2011.
7. Kim, D.-O., N.-I. Jo, H.-A. Jang, and C.-Y. Kim, "Design of the ultrawideband antenna with a quadruple-band rejection characteristics using a combination of the complementary split ring resonators," *Progress In Electromagnetics Research*, Vol. 112, 93–107, 2011.
8. Saleem, R. and A. K. Brown, "Empirical miniaturization analysis

of inverse parabolic step sequence based UWB antennas," *Progress In Electromagnetics Research*, Vol. 114, 369–381, 2011.

9. Chen, Z., Y. L. Ban, J. H. Chen, J. L. W. Li, and Y. J. Wu, "Bandwidth enhancement of LTE/WWAN printed mobile phone antenna using slotted ground structure," *Progress In Electromagnetics Research*, Vol. 129, 469–483, 2012.
10. Lin, D. B., I. T. Tang, and M. Z. Hong, "A compact quad-band PIFA by tuning the defected ground structure for mobile phones," *Progress In Electromagnetics Research B*, Vol. 24, 173–189, 2010.
11. Li, C. M. and L. H. Ye, "Improved dual band-notched UWB slot antenna with controllable notched bandwidths," *Progress In Electromagnetics Research*, Vol. 115, 477–493, 2011.
12. Zhou, D., S.-C. S. Gao, F. Zhu, R. A. Abd-Alhameed, and J.-D. Xu, "A simple and compact planar ultra wideband antenna with single or dual band-notched characteristics," *Progress In Electromagnetics Research*, Vol. 123, 47–65, 2012.
13. Liu, J., K. P. Esselle, S. G. Hay, and S.-S. Zhong, "Study of an extremely wideband monopole antenna with triple band-notched characteristics," *Progress In Electromagnetics Research*, Vol. 123, 143–158, 2012.
14. Lamultree, S. and C. Phongcharoenpanich, "Bidirectional ultra-wideband antenna using rectangular ring fed by stepped monopole," *Progress In Electromagnetics Research*, Vol. 85, 227–242, 2008.
15. Yu, A., F. Yang, and A. Elsherbeni, "A dual band circularly polarized ring antenna based on composite right and left handed metamaterials," *Progress In Electromagnetics Research*, Vol. 78, 73–81, 2008.
16. Chen, Y., S. Yang, and Z.-P. Nie, "A novel wideband antenna array with tightly coupled octagonal ring elements," *Progress In Electromagnetics Research*, Vol. 124, 55–70, 2012.
17. Pues, H. G. and A. R. Van De Capelle, "An impedance matching technique for increasing the bandwidth of microstrip antennas," *IEEE Trans. Antennas and Propagation*, Vol. 37, No. 11, 1345–1354, 1989.
18. Wong, K. L. and T. W. Kang, "GSM850/900/1800/1900/UMTS printed monopole antenna for mobile phone application," *Microwave Opt. Technol. Lett.*, Vol. 50, 3192–3198, 2008.
19. Ban, Y. L., J. H. Chen, L. J. Ying, J. L. W. Li, and Y. J. Wu, "Ultra wideband antenna for LTE/GSM/UMTS wireless USB dongle applications," *IEEE Antennas and Wireless Propagation*

Letters, Vol. 11, 403–406, 2012.

20. Islam, M. T., R. Azim, and A. T. Mobashsher, "Triple band-notched planar UWB antenna using parasitic strips," *Progress In Electromagnetics Research*, Vol. 129, 161–179, 2012.
21. Gujra, M., J. L.-W. Li, T. Yuan, and C.-W. Qiu, "Bandwidth improvement of microstrip antenna array using dummy EBG pattern on feedline," *Progress In Electromagnetics Research*, Vol. 127, 79–92, 2012.
22. Deng, J., L. Guo, T. Fan, Z. Wu, Y. Hu, and J. Yang, "Wideband circularly polarized suspended patch antenna with indented edge and gap-coupled feed," *Progress In Electromagnetics Research*, Vol. 135, 151–159, 2013.
23. Alvarez-Folgueiras, M., J. A. Rodriguez-Gonzalez, and F. Ares-Pena, "Experimental results on a planar array of parasitic dipoles fed by one active element," *Progress In Electromagnetics Research*, Vol. 113, 369–377, 2011.
24. Zhu, F., S.-C. S. Gao, A. T. S. Ho, C. H. See, R. A. Abd-Alhameed, J. Li, and J.-D. Xu, "Design and analysis of planar ultra-wideb and antenna with dual band-notched function," *Progress In Electromagnetics Research*, Vol. 127, 523–536, 2012.
25. Chang, T. N. and J. H. Jiang, "Enhance gain and bandwidth of circularly polarized microstrip patch antenna using gap-coupled method," *Progress In Electromagnetics Research*, Vol. 96, 127–139, 2009.
26. Elsheakh, D. N., H. A. Elsadek, and E. A. Abdallah, "Ultra-wide bandwidth microstrip monopole antenna by using electromagnetic band-gap structures," *Progress In Electromagnetics Research Letters*, Vol. 23, 109–118, 2011.
27. Zulkifli, F. Y., F. Narpati, and E. T. Rahardjo, "S-shaped patch antenna fed by dual offset electromagnetically coupled for 5–6 GHz high speed network," *PIERS Online*, Vol. 3, No. 2, 163–166, 2007.
28. Zhou, B., H. Li, X. Zou, and T.-J. Cui, "Broadband and high-gain planar Vivaldi antennas based on inhomogeneous anisotropic zero-index metamaterials," *Progress In Electromagnetics Research*, Vol. 120, 235–247, 2011.
29. Zhao, F., K. Xiao, W. J. Feng, S. L. Chai, and J. J. Mao, "Design and manufacture of the wideband aperture-coupled stacked microstrip antenna," *Progress In Electromagnetics Research C*, Vol. 7, 37–50, 2009.
30. Lai, C. H., "Broadband aperture-coupled microstrip antennas with low cross polarization and back radiation," *Progress In*

Electromagnetics Research Letters, Vol. 5, 187–197, 2008.

31. Lien, H. C., H. C. Tsai, Y. Lee, and W. F. Lee, "A circular polarization microstrip stacked structure broadband antenna," *PIERS Online*, Vol. 4, No. 2, 259–262, 2008.
32. Ollikainen, J., M. Fischer, and P. Vainikainen, "Thin dual-resonant stacked shorted patch antenna for mobile communications," *Electronics Letters*, Vol. 35, 437–438, 1999.
33. Zaid, L., G. Kossiavas, J. Y. Dauvignac, J. Cazajous, and A. Papiernik, "Dual-frequency and broad-band antennas with stacked quarter wavelength elements," *IEEE Trans. Antennas and Propagation*, Vol. 47, No. 4, 654–660, 1999.
34. Chen, Y., S. Yang, and Z. Nie, "Bandwidth enhancement method for low profile E-shaped microstrip patch antennas," *IEEE Trans. Antennas and Propagation*, Vol. 58, No. 7, 2442–2447, 2010.
35. Bahal, I. J. and P. Bhartia, *Microstrip Antenna*, Artech House, Massachusetts, 1980.
36. Pozar, D. M. and D. H. Schaubert, *Microstrip Antennas, the Analysis and Design of Microstrip Antennas and Arrays*, IEEE Press, New York, 1995.
37. Chen, Y. and C. F. Wang, "Characteristic-mode-based improvement of circularly polarized U-slot and E-shaped patch antennas," *IEEE Antennas and Wireless Propagation Letters*, Vol. 11, 1474–1477, 2012.
38. Wu, W. and Y. P. Zhang, "Analysis of ultra-wideband printed planar quasi-monopole antennas using the theory of characteristic modes," *IEEE Antennas Propag. Mag.*, Vol. 52, No. 6, 67–77, 2010.